LA-UR-18-25097
Approved for public release; distribution is unlimited.

Title: Supo Thermal Model Development III

Author(s): Wass, Alexander Joseph

Intended for: Report

Issued: 2018-06-11

**Introduction**

This report describes the continuation of the Computational Fluid Dynamics (CFD) model of the Supo cooling system described in the reports, Supo Thermal Model Development[1] and Supo Thermal Model Development II[2]. The goal for this report is to more accurately estimate the natural convection heat transfer coefficient (HTC) of the system using the CFD results and to compare those results to remaining past operational data.

In the previous report[2], twenty cases (power levels) from the Durham and Bunker reports were modeled using the appropriate boundary conditions and material properties determined using the experiment results for each individual power level. The laminar flow model over-predicted the natural convection HTC for the lowest power density experimental data point by 479% and under-predicted the HTC for the highest power density experimental data point by 40%. In order to improve these results, CFD simulations are modeled using laminar and turbulent flow regimes according to the power density in which the HTC needs improvement. This includes maintaining a laminar fluid model with zero radiolytic gas generation at power densities below 0.884 kW/L and using a turbulent model at higher power densities above 0.884 kW/L.

**Supo History and CFD Model**

Supo, or "Super-Power" was a 45 kW water boiler reactor that consisted of a uranyl-nitrate solution within a spherical vessel. Supo was operated from 1951 to 1974 at what is currently called Los Alamos National Laboratory. The vessel contained water-cooled spiral coils distributed throughout the solution to maintain desired operating temperatures, re-entrant thimbles containing boron control rods, and a "glory hole" allowing neutron data to be acquired. Supo was mainly used for neutron research, and proved to be a versatile and reliable research tool.

The CFD geometry and 2-D axisymmetric mesh of Supo remained unchanged from the previous reports[1,2]. Buechler's report[1] and the previous report[2] contains detailed information on the background and setup of this work, which are extracted from reports by King[3], Durham[4], and Bunker[5]. Figure 1 shows a sketch of Supo containing the internal components such as the cooling tubes and liquid level[5].

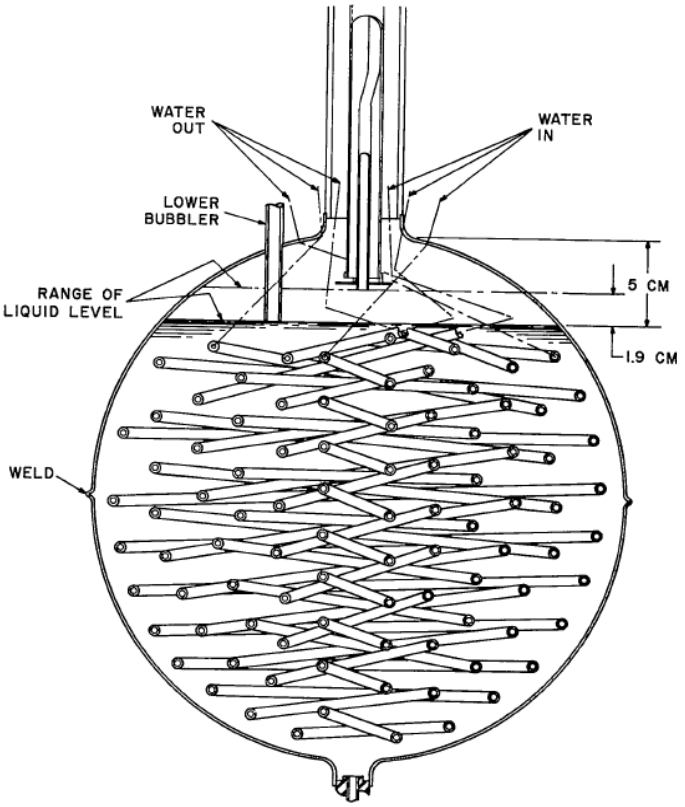


**Figure 1 –** Cross sectional sketch of the internal components in the Supo reactor vessel[5]

[1] C. Buechler, LA-UR-16-29483, Supo Thermal Model Development, 2016.

[2] A. Wass, LA-UR-17-25822, Supo Thermal Model Development II, 2017.

[3] L. D. P. King, Design and Description of Water Boiler Reactor, Proceedings of the International Conference on the Peaceful Uses of Atomic Energy, 1955

[4] F. Durham, Radiolytic-Gas Bubbling Improves Convective Heat Transfer in Supo, Nucleonics, 1955.

[5] M.E. Bunker, Status Report on the Water Boiler Reactor, LA-2854, 1963.

The material properties, heat and mass generation profiles, and wall boundary conditions are the same from the previous report[2]. However, the report by Buechler[1] explains the process for determining these model inputs in greater detail. Properties were determined for each power level using the appropriate fluid temperatures determined by Durham's and Bunker's experiment results[4,5]. Buechler[1] also determined temperature-dependent polynomials of the radiolytic gas mixture properties[6] for density, specific heat, thermal conductivity, viscosity, and molecular mass using mass fractions of $H_2$ and $O_2$.

The power and mass generation profiles were modeled as a spherically-symmetric Gaussian profile within the solution portion of the vessel. Buechler determined these profiles from assumptions and examples in King's and Bunker's reports[3,5,7]. Such assumptions included a power deposition in the liquid proportional to the neutron flux. A plot of the power deposition profile ($W/m^3$) that was used for the 3.05 kW/L (40 kW) case is show in Fig. 2. One should note that the peak power is higher in order to achieve the desired volume integrated power of Supo. The mass source was introduced as a mixture of oxygen and hydrogen and proportional to the reactor power and power deposition profile.

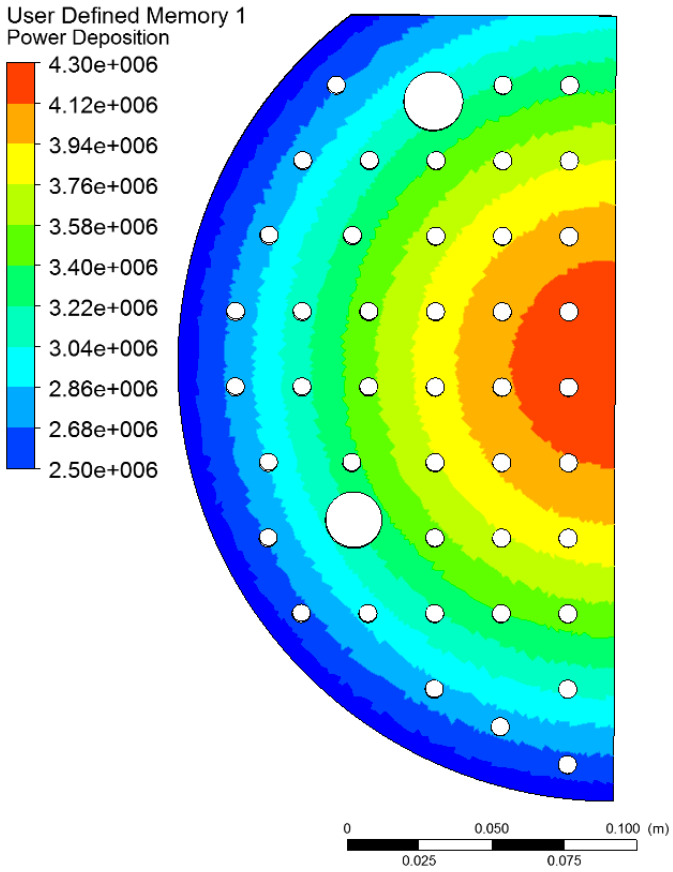


**Figure 2 -** Power deposition profile (W/m3) for the 3.05 kW/L (40 kW) case

**Natural Convection Model**

The fluid flow of the fuel solution was modeled in the commercial CFD software, ANSYS Fluent, Version 18.2. An important part of the CFD setup is to determine what flow regime to use. In the previous report[2], the fluid flow regime was defined as laminar based on the Rayleigh number that describes the buoyancy-driven flow within the vessel. Rayleigh numbers were calculated for each case from the Bunker and Durham reports[4,5], and were orders of magnitude smaller than the value at which transition to turbulence is expected ($10^9$). Although, the Rayleigh number does not account for the mixing enhancements from the rising gas bubbles. The previous simulation results suggested that a laminar flow regime might only be applicable at low power densities, while a turbulent flow regime might be better used at higher power densities due to the additional bubble mixing enhancements.

The results from the previous report[2] showed that at power densities below 0.884 kW/L, the simulation free convection HTC over-predicted the experiment values by up to 479%. It was hypothesized that the radiolytic gas may have been soluble in the solution, and not formed bubbles. Thus, in order to decrease the mixing enhancements due to bubbles, gas generation was turned off for these three cases (0.290, 0.293, and 0.439 kW/L). For power densities above 0.884 kW/L, the previous results[2] under-predicted the experiment calculated HTC by as much as 41%.

[6] Incropera and DeWitt, Fundamentals of Heat and Mass Transfer, 4th Ed., Wiley, 1996, p. 841-842.

[7] King, et. al., Gas Recombination System for a Homogeneous Reactor, Nucleonics, Vol. 11, No. 9, 1953.

Since the gas bubbles were determined to create turbulent wakes, a turbulent flow model was used to increase the HTC closer to the experimentally determined values.

The laminar flow models within Fluent remained the same from the previous report[2], except that bubble generation was set to zero. The k-omega SST turbulent model with dispersed turbulence multiphase option was recommended by ANSYS and was introduced in this work. Most of the bubble phase interaction models remained the same in this report as previously defined. The bubble drag model was set as the Schiller-Naumann drag model, the bubble lift force and vertical wall effects were modeled using the Tomiyama lift force and Antal wall lubrication force models, respectively, and the multi-phase heat transfer was modeled using the Ranz-Marshall heat transfer model. Two turbulent based models were required for the multiphase, turbulent cases. The turbulent dispersion model was set as the Burns dispersion model, and the turbulence interactions were modeled using the Sato model.

**Model Parameters and Solution Methods**

Similar to the previous report, the same model parameter and solution methods were used for each case from the Durham[4] and Bunker[5] reports. Also, the boundary conditions for each case remained unchanged. The results were considered fully converged when the power balance between the cooling tubes and the outer wall matched the total power generation to within 1%. Like before, the CFD results fluctuated by as much as 1% of its steady-state value so the results were averaged to at least 10,000 iterations to produce steady-state result values for each case. The mass flow of bubbles at the degassing boundary condition, maximum and average solution temperatures, cooling tube power and tube temperature, and volume fraction were also averaged.

**Bubble Size Determination**

The method for determining radiolytic gas bubble size remained the same from the previous work[2]. The bubble size was determined using experimental values from King's and Bunker's reports[3,5], as well as two bubble diameters measured at Argonne National Laboratory by Chemerisov et al.[8] A linear relationship between bubble diameter and power density was developed that results in positive values for bubble diameter at all power densities, as shown in Fig. 3. The predicted bubble diameter is: Bubble diameter (mm) = 0.652*(Power density in kW/L) + 0.1099.

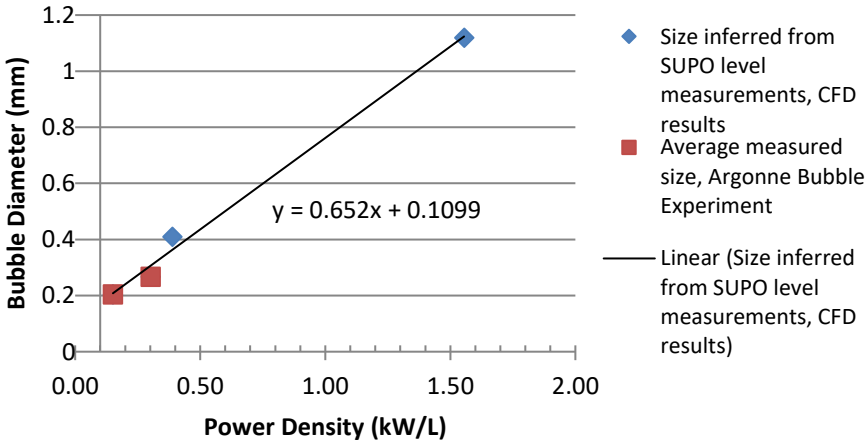


**Figure 3 -** Linear fit of bubble diameter using measured data and CFD results

[8] Chemerisov et al., Experimental Results for Direct Electron Irradiation of a Uranyl Sulfate Solution: Bubble Formation and Thermal Hydraulics Studies, ANL/NE-15/19.

**Results**

The same cases from the previous report[2] were modeled in this work. This includes data from Durham's Group A through C experiments[4], as well as Bunker's single experiment at 25.173 kW[5]. Like before, the Durham Group B, 3.2 kW (0.24 kW/L) case, was not simulated due to a non-physical energy balance calculated from the results reported in the Durham report. Also, five remaining cases with reactor powers between 25.2 and 39.2 kW were not simulated because the group for each case was not defined in the Durham report[4], and the boundary conditions for each case could not be accurately determined without this information.

The tabulated simulation results and corresponding boundary conditions for the Durham and Bunker cases can be seen in Table 1, and are organized by flow regime and phase. The boundary conditions shown in this table include the bubble diameter, cooling tube inside HTC and free stream temperature. The resulting average solution temperature, bubble volume fraction, and natural convection HTC are shown as well. Further explanation of the results is provided in the following sections.

**Table 1:** Calculations and CFD results for Durham and Bunker cases separated by flow regime

| Power (kW) | Power Density (kW/L) | Bubble Diameter (mm) | Tube Inside (forced convection) HTC ($W/m^2$-K) | Tube Inside Free Stream Temp (°C) | Volume-Avg Solution Temp Result (°C) | Volume-Avg Volume Fraction Result | Tube Outside (natural convection) HTC Result ($W/m^2$-K) | Experiment HTC Result ($W/m^2$-K) |
|---|---|---|---|---|---|---|---|---|
| Laminar, single phase, zero bubble generation | | | | | | | | |
| 3.8 | 0.290 | 0 | 597 | 36.0 | 57.7 | 0 | 978 | 312 |
| 3.85 | 0.293 | 0 | 6537 | 27.9 | 43.6 | 0 | 832 | 355 |
| 5.76 | 0.439 | 0 | 6089 | 35.9 | 52.4 | 0 | 978 | 799 |
| Laminar, multiphase | | | | | | | | |
| 11.6 | 0.884 | 0.838 | 11,139 | 33.1 | 54.0 | 0.00581 | 2045 | 1997 |
| Turbulent, multiphase | | | | | | | | |
| 17.15 | 1.31 | 0.962 | 17,552 | 33.7 | 52.2 | 0.00700 | 3893 | 2644 |
| 23.1 | 1.76 | 1.258 | 24,828 | 32.1 | 54.4 | 0.00835 | 4234 | 2824 |
| 25.173 | 1.92 | 1.361 | 20,285 | 17.9 | 50.2 | 0.00886 | 4057 | 2907 |
| 25.2 | 1.92 | 1.362 | 21,256 | 28.0 | 59.2 | 0.00876 | 4125 | 2754 |
| 25.8 | 1.97 | 1.392 | 24,027 | 34.1 | 58.6 | 0.00889 | 4369 | 3129 |
| 30.4 | 2.32 | 1.620 | 25,879 | 33.9 | 65.8 | 0.00981 | 4405 | 3463 |
| 30.8 | 2.35 | 1.641 | 22,997 | 32.5 | 69.5 | 0.00980 | 4379 | 3371 |
| 31.2 | 2.38 | 1.660 | 22,430 | 31.8 | 68.9 | 0.00999 | 4401 | 3262 |
| 31.3 | 2.39 | 1.665 | 26,086 | 34.6 | 67.1 | 0.00999 | 4442 | 3324 |
| 31.6 | 2.41 | 1.680 | 22,474 | 32.5 | 70.3 | 0.0101 | 4425 | 3608 |
| 36.6 | 2.79 | 1.929 | 23,898 | 35.0 | 76.8 | 0.0111 | 4643 | 3961 |
| 37.3 | 2.84 | 1.964 | 27,445 | 36.8 | 73.9 | 0.0112 | 4669 | 4048 |
| 38 | 2.90 | 1.998 | 28,138 | 37.5 | 74.3 | 0.0114 | 4739 | 3903 |
| 38.6 | 2.94 | 2.028 | 24,172 | 35.0 | 78.9 | 0.0115 | 4693 | 4186 |
| 38.9 | 2.96 | 2.043 | 23,654 | 34.0 | 78.0 | 0.0116 | 4687 | 3949 |
| 40 | 3.05 | 2.098 | 28,539 | 39.3 | 78.0 | 0.0118 | 4821 | 4445 |

**Heat Transfer Coefficient Results**

The natural convection heat transfer coefficient was calculated from the CFD results for each case, based on the difference between the volume-average fuel temperature, $T_f$, and the average temperature of the cooling tube outer surfaces, $T_{s,o}$:

$$\bar{h}_{o,CFD} = \frac{q}{A_o(T_f - T_{s,o})}.$$

Figure 4 shows the natural convection heat transfer coefficients for the Durham and Bunker experimental data compared to the results calculated from the simulation data for each operating condition. The simulation result HTC values are provided from both the previous work[2] (laminar flow model with bubble generation) and the current work (laminar flow model without bubbles and turbulent flow model with bubbles). At power densities below 0.884 kW/L, the simulation natural convection HTC using a laminar model without bubbles provides a much better prediction of the experimental value. The HTC values predicted using the single-phase, laminar simulations are 22-214% greater than the experiment values, which is an improvement of about 50% over the multi-phase, laminar simulations performed in the previous work[2]. Between power densities of 1.31 and 2.41 kW/L, the free convection HTC predictions of the turbulent simulations show poorer agreement with the experiment than the laminar simulations. The turbulent simulation HTC results over-predicted the experiment results by 23-47%, whereas the laminar simulations under-predicted the HTC by 17-32%. Above 2.41 kW/L, the turbulent simulation HTC results show much better agreement with experiment than the previous laminar simulations. The turbulent CFD simulation HTC results over-predicted the experiment results by 8.5-21%, whereas the laminar simulations under-predicted the HTC by 34-41%.

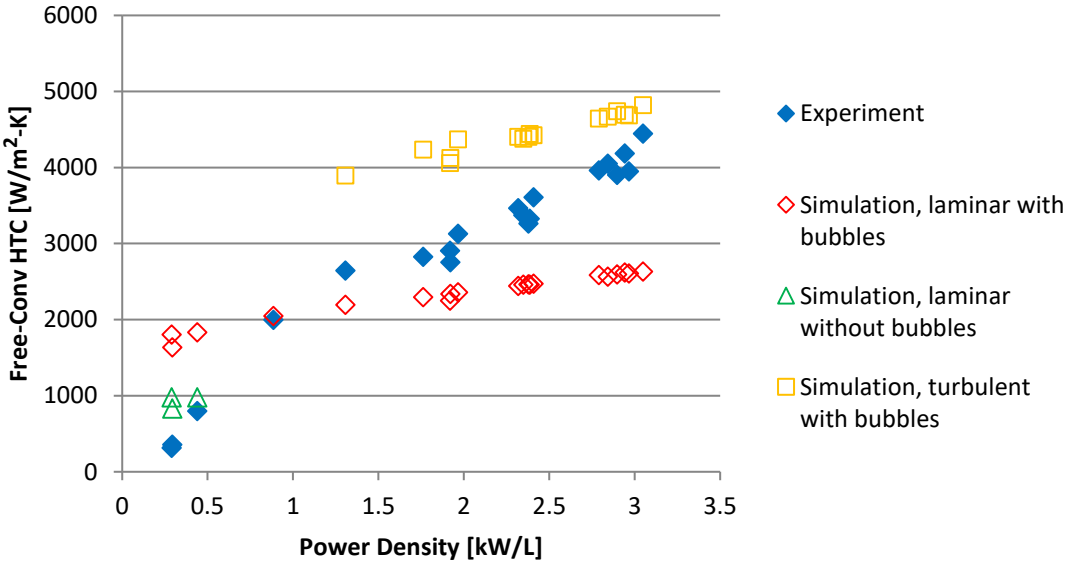


**Figure 4 –** Experiment-calculated heat transfer coefficients compared with simulation results

Figure 5 shows the experiment and simulation results compared to the heat transfer coefficients calculated using the correlation with the Morgan coefficients described in the previous reports[1,2]. The Morgan correlation is only valid for single phase flow, so it does not include the additional mixing enhancements of the radiolytic gas bubbles. Therefore, the HTC result is much lower than what was determined from most of the experiments and the multi-phase flow simulations. This correlation also makes use of the Rayleigh number, which requires temperatures for the cold tube wall and the hot liquid, determined via simulation.

In the previous work[2], it was determined that the HTC correlation using Morgan coefficients far underestimated the HTC results from both the experiment and simulation at power densities greater than 0.884 kW/L. Nevertheless, at power densities less than 0.884 kW/L, the Morgan correlation proved more suitable for determining HTC. In this work, the HTC determined from the Morgan correlation was within 3% of the single-phase laminar simulation results. This was an expected result since single phase flow was used in these cases where the Morgan correlation is valid.

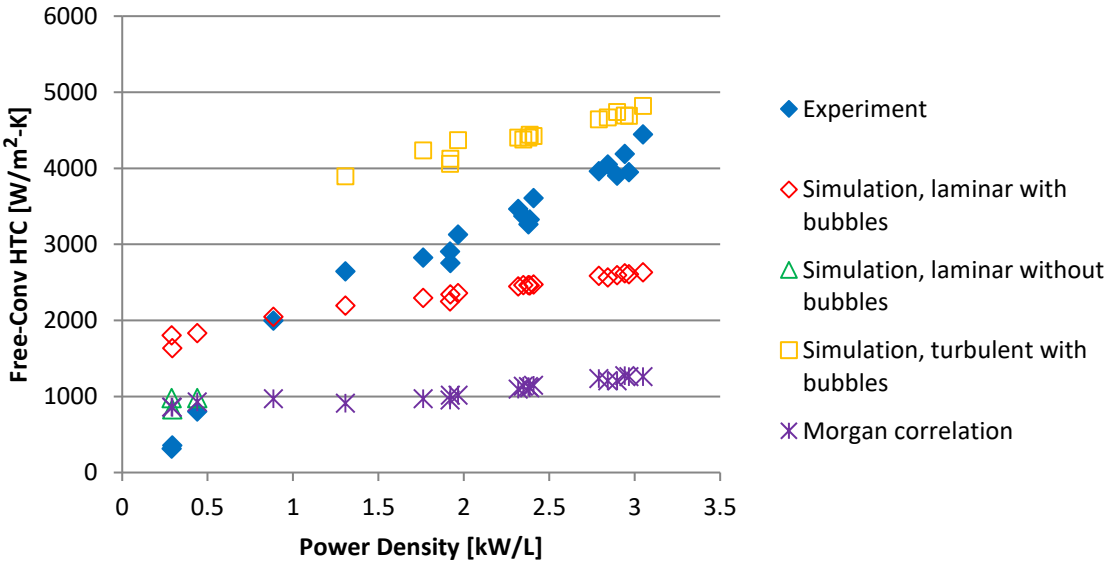


**Figure 5 -** Simulation HTC results compared with correlation HTC values

**Temperature Results**

The experimental solution temperatures were provided in reports by Durham[4] and Bunker[5], and compared to the average solution temperature resulting from the simulations. The solution temperature in the simulations was taken as an average since there was no evidence provided in the Bunker and Durham reports that described how or where the solution temperature was recorded. Figure 6 shows this comparison for simulations using single and multi-phase laminar and multiphase turbulent flow models.

The average solution temperature simulation results using the laminar flow model from the previous work[2] showed increasingly higher temperatures over the experiment at power densities above 1.31 kW/L. The temperature simulation results in this work using a turbulent model under-predict the experimentally measured temperature above 0.884 kW/L. Temperature differences as large as 13°C were obtained, compared to 8.6°C for the laminar flow model. However, this work showed an improvement in temperature difference compared to the experiment at power densities below 0.884 kW/L. The CFD simulations using the laminar fluid model without bubble generation resulted in temperature differences between 7.7 and 19°C, whereas the simulations using the laminar model with bubble generation showed greater differences of 14 to 25°C.

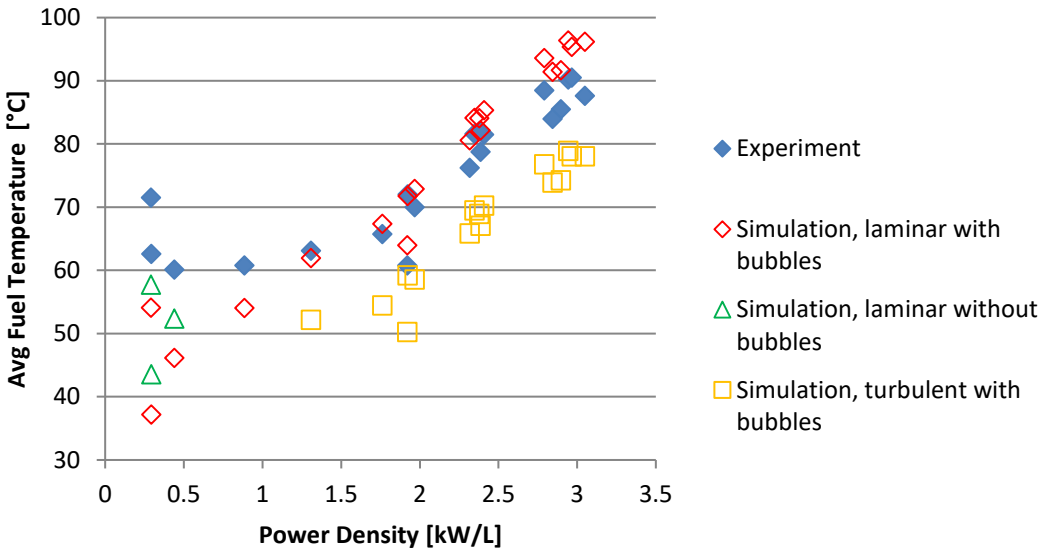


**Figure 6 -** Average fuel temperature for experimental data and simulation results

One will notice that at a power density of 0.884 kW/L, the CFD simulation and the experimentally calculated HTC match very closely in Fig 4. However, in Fig. 6, the average fuel temperature at this same power density is about 6.7°C less than the experiment value. Thus, the experimental and CFD simulation fuel temperature does not match even when the free convection HTC is similar. One reason, upon several others, is due to how ANSYS Fluent calculates wall temperature. The cooling tube wall resistance is calculated assuming a plane wall and not a cylindrical wall. This, in turn, causes some error between the expected cooling tube surface temperature result and the determined result from Fluent, along with other slight variations in the way Fluent determines temperature.

A comparison of the solution temperature profiles for the 3.05 kW/L (40.0 kW) case using the laminar (left) and turbulent (right) flow models is shown in Fig. 7. As expected, the case using the laminar model has a higher average temperature than the turbulent flow model, and the average temperature relative to the maximum temperature is lower than the turbulent model. The liquid circulation pattern is similar for both models. Like previously, the highest fuel temperature for both flow models is observed above the glory hole where the center of rotation is believed to be located. The liquid in this region is nearly stagnant which leads to poor heat transfer, thus, increased temperature occurs. Interestingly, the turbulent model also contains a high temperature region near the bottom of the vessel, unlike in the laminar model.

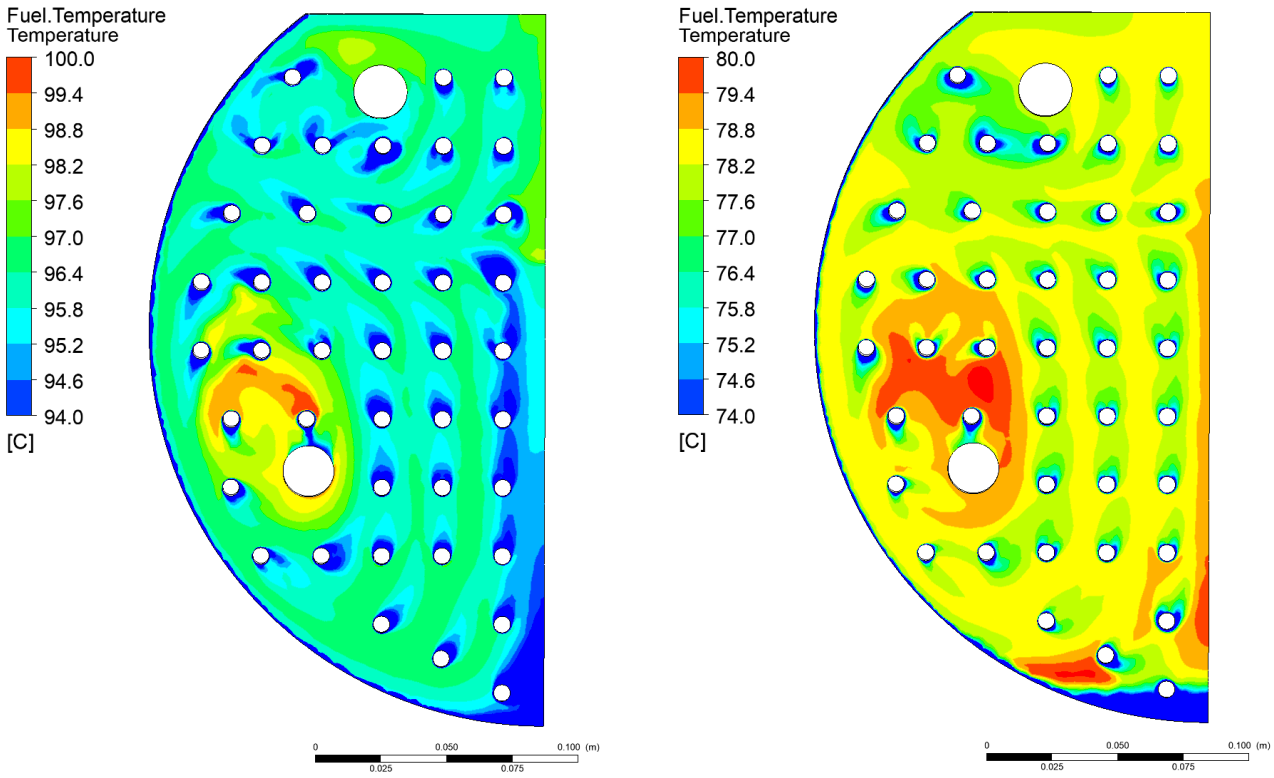


**Figure 7 -** Temperature profile for the 3.05 kW/L laminar (left) and turbulent case (right)

**Bubble Distribution Results**

Figure 8 shows contours of the bubble volume fraction distribution for the turbulent 3.05 kW/L case. The distribution is similar to the results from the previous work[2]. The volume-average bubble volume-fraction is 0.0118 for this case. Like before, greater bubble volume fractions can be seen near the top of Supo where the bubbles rise due to buoyant forces. The volume fraction steadily decreases further down the solution vessel. The average bubble volume fraction for the remaining Durham and Bunker cases was shown previously in Table 1.

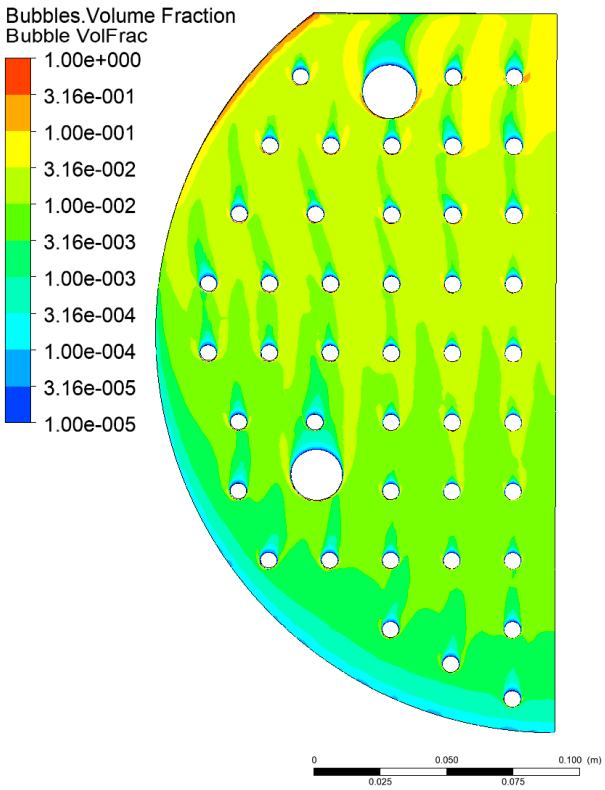


**Figure 8 -** Bubble volume fraction profile for 3.05 kW/L turbulent case

**Velocity Results**

Vertical fuel and bubble velocity contour plots are shown in Fig. 9. Throughout the vessel, the gas bubbles rise much faster than the solution since the density difference between the two fluids is large. The fuel solution in Supo flows in a “figure 8” pattern. The solution flows in a counter-clockwise motion about the glory hole near the bottom of the vessel, and clockwise around the control rod thimble towards the top. One can see this flow pattern in more detail from the velocity vector plot for the turbulent 3.05 kW/L case in Fig. 10.

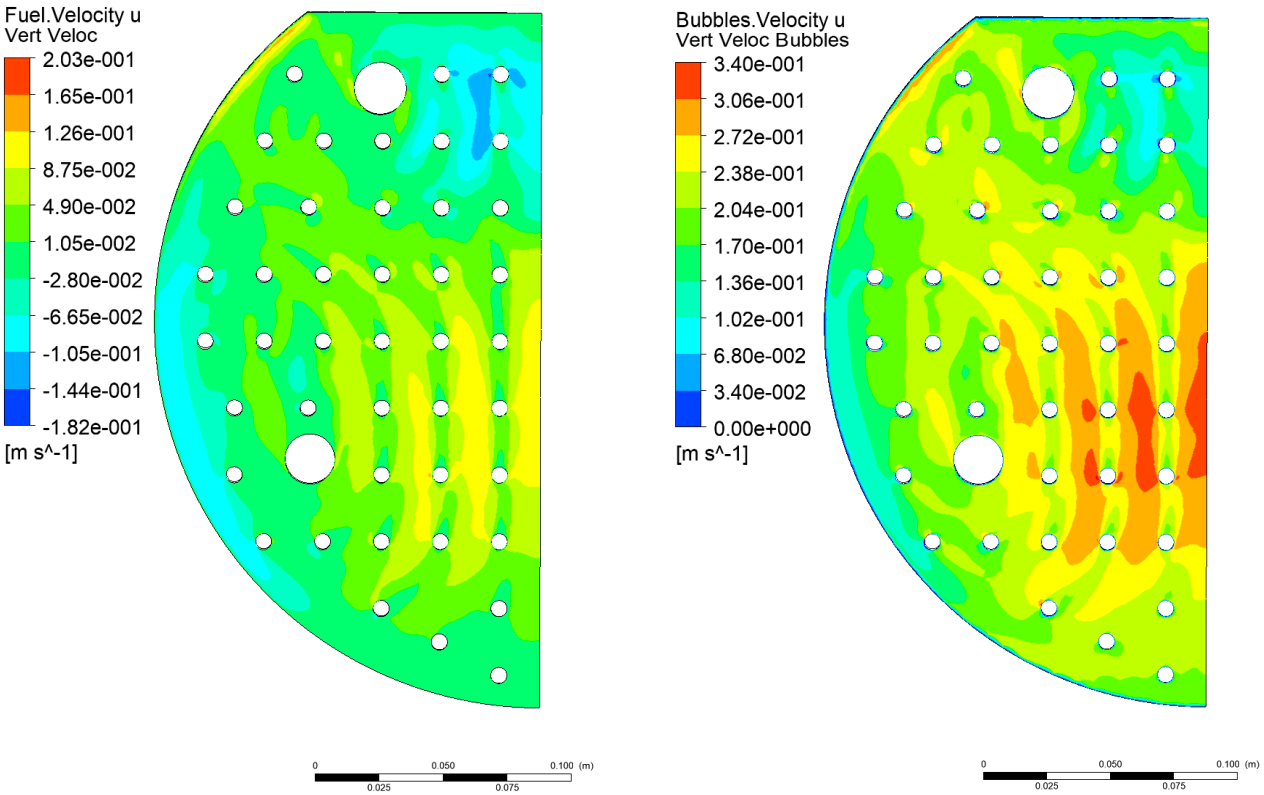


**Figure 9 -** Vertical velocity contours of fuel (left) and gas bubbles (right) for the 3.05 kW/L turbulent case

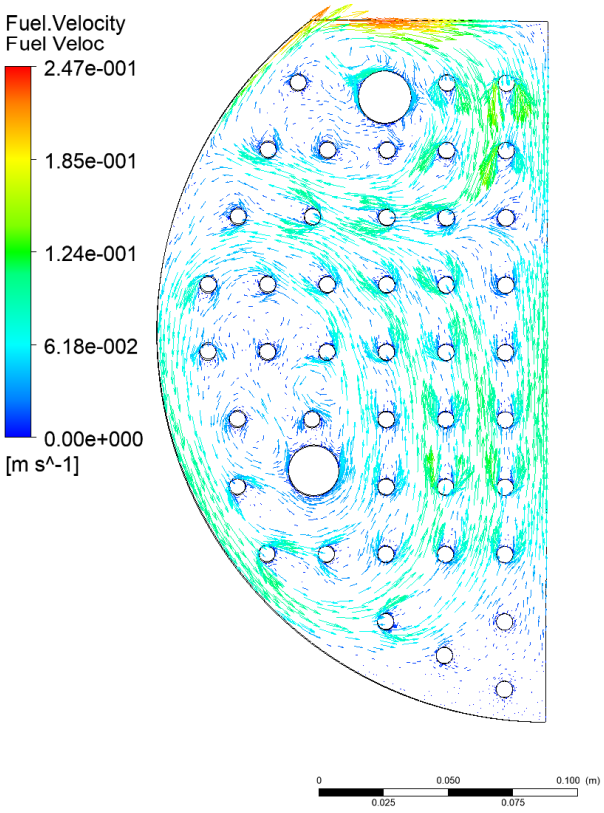


**Figure 10 -** Velocity vectors (left) for the turbulent 3.05 kW/L case

The Reynolds number is used in convection fluid flow problems to determine if the boundary layer around certain objects is laminar, turbulent, or in a transition state. The radiolytic gas bubbles generated in the solution achieve velocities relative to the solution that resemble forced convective flows. Fluid flow around the radiolytic gas bubbles was analyzed using the Reynolds number assuming a spherical geometry. The average Reynolds number of the flow around a sphere is calculated by:

$$\overline{Re}_D = \frac{\rho D V}{\mu},$$

where $D$ is the sphere diameter, and $V$ is the liquid velocity past the sphere. The density and viscosity were taken at the average solution temperature. For Reynolds numbers between 10 and 1000, a sphere will exhibit a laminar boundary layer that separates from the surface, and eddies will form in its wake[9]. Some turbulence will exist behind the rising bubbles, contributing to mixing. A fully-developed turbulent wake will be

[9] Street et. al., Elementary Fluid Mechanics, 7th Ed., Wiley, 1996, p. 500-502.

present at Reynolds numbers above 1000. This turbulence is deliberately modeled in this work unlike the laminar flow model used for Supo in the previous work[2].

Velocity for this calculation was determined using the relative volume average vertical bubble velocity. It is shown for the turbulent 3.05 kW/L case in Fig. 11 that the relative vertical bubble velocity is nearly uniform throughout Supo. Hence, an average relative bubble velocity is a good assumption for solving bubble Reynolds number. The volume average relative vertical bubble velocity for this case is 0.206 m/s (compared to 0.208 m/s using a laminar flow model).

Figure 12 shows the Reynolds number of the bubbles, or particles, using the simulation results for each Bunker and Durham case. The results show that the particle Reynolds number for the turbulent cases do not exceed the fully developed turbulent value of 1000, unlike the simulations using the laminar flow model. The cause of these low values is due to the temperature dependent solution viscosity and density. Since the average solution temperature was lower in the turbulent simulations, the solution viscosity was calculated to be higher using the temperature-dependent correlation. This resulted in about half the particle Reynolds number at high power densities.

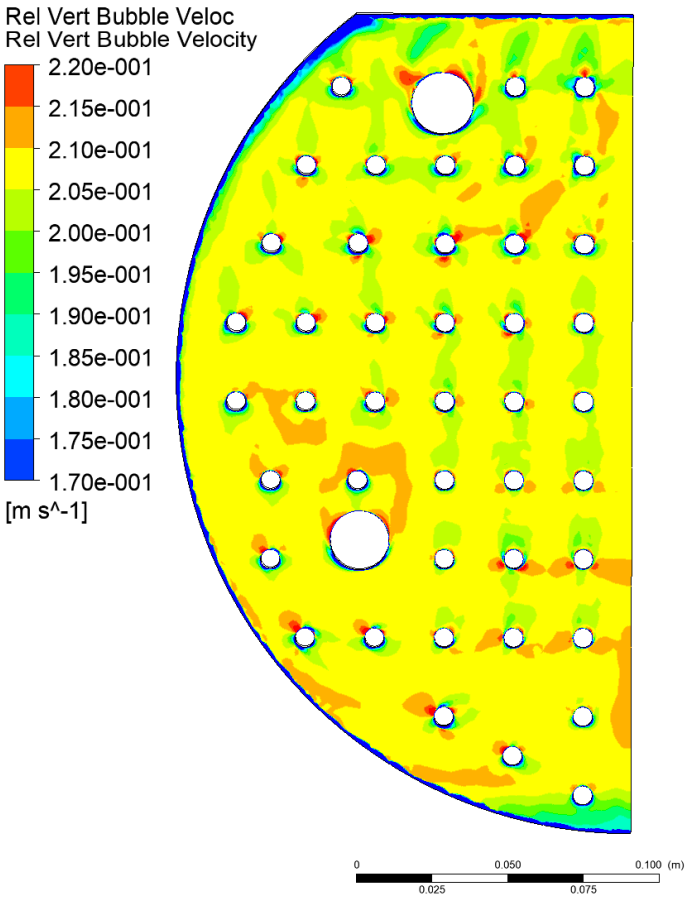


**Figure 11 -** Relative vertical bubble velocity for the turbulent 3.05 kW/L case

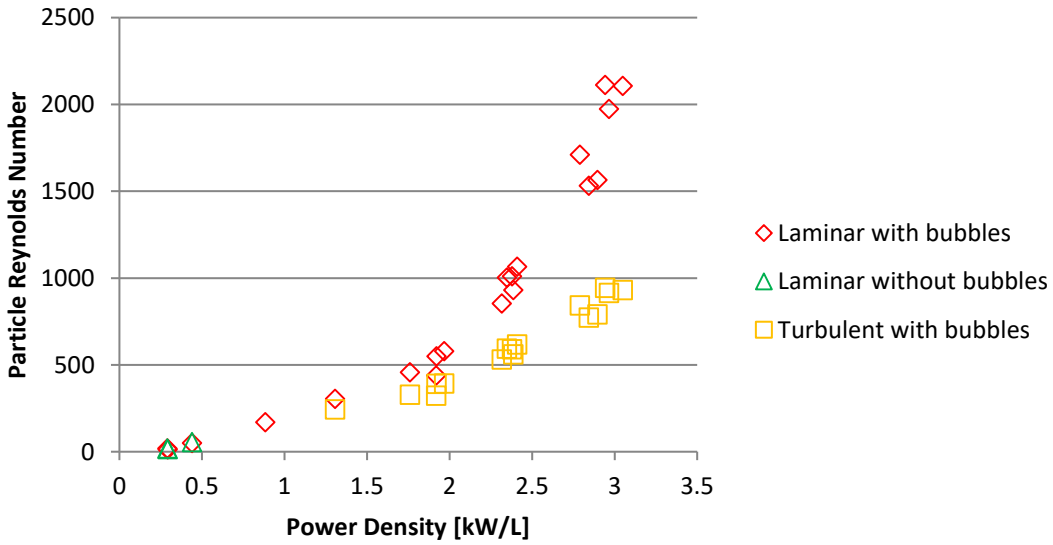


**Figure 12 -** Particle Reynolds number calculated from simulation results

**Conclusion**

The single-phase, laminar flow model reduced the natural convection HTC at low power densities by about 50%. At 0.439 kW/L, the CFD simulation HTC result matched the experiment HTC calculation to within 22%. However, differences as high as 214% were still present at the lowest powers. Nonetheless, this fluid model provides the best result yet at low power densities. The multi-phase, turbulent flow model improved the HTC at the highest power densities and was as close as 8.5% from the experiment. Again, this choice of fluid models is the most appropriate for these power densities. Slightly larger differences between the multi-phase turbulent flow results and the experimentally determined HTC values were seen in the mid-range power densities. The difference between the CFD simulation HTC results and the experimentally calculated HTC in this range was as low as 23% and as high as 47%. It appears that this range of power densities contains laminar to turbulent transitional flow. Results from the laminar and turbulent models bound the experimentally measured data, but neither model accurately predicts the system behavior at all power levels.

**Future Work**

Requests have been made to perform future simulations of cases from this report using a 3-D geometry, instead of a 2-D, axisymmetric geometry. Supo contains several non-symmetric components that are currently modeled symmetrically and may affect the natural convection HTC results. The importance of this is to determine how much the results change, and if the 2-D CFD simulation results are valid.